Reversal of Hypertriglyceridemia, Fatty Liver Disease and Insulin Resistance by a Liver-Targeted Mitochondrial Uncoupler

Rachel J. Perry[1,2,3], **Taehan Kim**[4], **Xian-Man Zhang**[1], **Hui-Young Lee**[1,3], **Dominik Pesta**[1], **Violeta B. Popov**[2], **Dongyan Zhang**[1], **Yasmeen Rahimi**[1], **Michael J. Jurczak**[1], **Gary W. Cline**[1], **David A. Spiegel**[4,5], and **Gerald I. Shulman**[1,2,3,6,*]

[1]Howard Hughes Medical Institute, Yale University School of Medicine New Haven, CT, USA 06519

[2]Department of Internal Medicine, Yale University School of Medicine New Haven, CT, USA 06519

[3]Department of Cellular & Molecular Physiology, Yale University School of Medicine New Haven, CT, USA 06519

[4]Department of Pharmacology, Yale University School of Medicine New Haven, CT, USA 06519

[5]Department of Chemistry, Yale University, New Haven, CT, USA 06520

[6]Novo Nordisk Foundation Center for Basic Biomedical Research Copenhagen, DK

Summary

Non-alcoholic fatty liver disease (NAFLD) affects one in three Americans and is a major predisposing condition for type 2 diabetes (T2D), however there are currently no drugs available to treat this disease. We examined whether a functionally liver-targeted derivative of 2,4-dinitrophenol (DNP), DNP-methyl ether (DNPME), could safely decrease hypertriglyceridemia, NAFLD and insulin resistance without systemic toxicities. Treatment with DNPME reversed hypertriglyceridemia, fatty liver and whole-body insulin resistance in high-fat fed rats and decreased hyperglycemia in a rat model of T2D with a wide therapeutic index. The reversal of liver and muscle insulin resistance was associated with reductions in tissue diacylglycerol content and reductions in PKCε and PKCθ activity in liver and muscle respectively. These results demonstrate that the beneficial effects of DNP on hypertriglyceridemia, fatty liver and insulin resistance can be dissociated from systemic toxicities and suggest the potential utility of liver-targeted mitochondrial uncoupling agents for the treatment of the related epidemics of NAFLD, metabolic syndrome and type 2 diabetes.

Introduction

Non alcoholic fatty liver disease (NAFLD) is a key factor in the pathogenesis of type 2 diabetes (T2D) and affects one in three Americans (Petersen et al., 2005; Shulman, 2000; Samuel and Shulman, 2012). NAFLD is also a key predisposing factor for the development of non-alcoholic steatohepatitis (NASH), cirrhosis and hepatocellular carcinoma. Furthermore it is anticipated that NAFLD-induced NASH will soon surpass hepatitis C and alcoholic cirrhosis as the most common indication for liver transplantation in the USA (Baffy et al., 2012; White et al., 2012). Therefore new and effective therapies for treatment of NAFLD are urgently needed.

In this regard we hypothesized that a liver-targeted mitochondrial uncoupling agent might be an effective and safe approach for the treatment of NAFLD and insulin resistance by promoting the oxidation of hepatic triglyceride, while avoiding hyperthermia and associated systemic toxicities that typically occur with classical mitochondrial uncoupling agents. One of the best characterized mitochondrial uncoupling agents is 2,4 dinitrophenol (DNP), a protonophore, which shuttles protons across the mitochondrial membrane dissipating the mitochondrial proton gradient resulting in the conversion of the energy derived from mitochondrial substrate oxidation to heat. DNP was extensively used as a weight loss remedy in the 1930s but taken off the market by the U.S. Food and Drug Administration in 1938 due to the occurrence of fatal hyperthermia (Tainter et al., 1934). Given that the toxicities of DNP are on-target effects related to systemic mitochondrial uncoupling, we hypothesized that the safety and therapeutic potential of DNP for treatment of NAFLD could be increased by targeting DNP to the liver. We therefore synthesized and screened liver-targeted DNP derivatives that would be preferentially metabolized by liver and converted to DNP. In this screen we found that DNP-methyl ether (DNPME) both prevented and reversed non-alcoholic fatty liver disease, insulin resistance and hyperglycemia in high-fat fed insulin resistance rat models of NAFLD, and T2D without hepatic or renal toxicity. These results demonstrate that the effects of DNP on hypertriglyceridemia, fatty liver and insulin resistance can be dissociated from systemic toxicities with a relatively wide therapeutic index and are proof of concept for developing liver-targeted mitochondrial uncoupling agents for the treatment of hypertriglyceridemia, NAFLD and type 2 diabetes.

Results and Discussion

We hypothesized that targeting DNP to the liver would reduce hypertriglyceridemia, hepatic lipid content and improve insulin sensitivity, without DNP-associated toxicities. We therefore generated several derivatives of DNP which we hypothesized would be preferentially metabolized by the cytochrome P-450 system in the liver to the active protonophore, DNP, and screened them in isolated hepatocytes for their ability to promote increased oxygen consumption (Fig. S1A–B). From this screen we identified two compounds, DNP-methyl ether (DNPME) and DNP-vinyl ether (DNPVE), which raised oxygen consumption rates in plated hepatocytes with similar potencies to DNP. We selected DNPME for further *in vivo* metabolic characterization studies due to its stability under acidic conditions, which would potentially allow oral administration. In contrast to DNP, which caused a large, dose-dependent increase in rectal temperatures and rapid dose-

dependent mortality at doses above 10 mg/kg, DNPME caused no such effects after an injection of up to 200 mg/kg (Fig. 1A–D). Consistent with these findings, we found that the LD_{50} dose of DNPME was almost tenfold higher than that of DNP (Fig. 1E). Five days of daily treatment with DNPME caused no appreciable hepatic or renal toxicity at daily doses below 50 mg/kg (Fig. 1F–I), but daily doses above 2.5 mg/kg were effective at reducing hepatic triglyceride accumulation in rats fed a high-fat diet and sucrose supplemented (5%) drinking water (Fig. 1J). In contrast, the toxic threshold of chronic DNP treatment was determined to be 1 mg/kg, whereas the lowest dose that was effective at lowering liver TAG was 5 mg/kg (Fig. S1C–G); thus the ratio of effective to toxic dose for DNP was 0.2 compared to 10 for DNPME. From these data we found that DNPME had a favorable therapeutic index (LD_{50}/ED_{50}) of 70 and selected the lowest effective daily dose of DNPME (5 mg/kg), which was tenfold lower than the minimal dose where we started to observe any indication of hepatic or systemic toxicities, to further characterize its effects on hepatic steatosis and insulin action *in vivo*. This therapeutic index compares favorably with other drugs that are in common use such as acetaminophen, which has a LD_{50}/ED_{50} of 13. Six weeks of daily treatment with DNPME at this dose caused no differences in liver or renal function tests, liver or renal histology, or rectal temperature (Fig. 1K–N, S1J–K).

The safety and efficacy profiles of DNPME led us to examine whether DNPME treatment could reverse pre-existing hypertriglyceridemia, hepatic steatosis and insulin resistance in a rat model of NAFLD. To this end, we induced hepatic steatosis in rats by feeding them a high fat diet with sucrose supplemented drinking water, and then treated them with DNPME or vehicle daily for 5 days. The rats treated with DNPME had lower fasting plasma glucose, triglyceride and insulin concentrations compared to the vehicle treated animals (Fig. 2A–C), despite identical body weight at the time of study, and identical food intake during the treatment period (S2A–B). Consistent with the reduced fasting plasma glucose and insulin concentrations DNPME-treated rats had a 20% reduction in basal endogenous glucose production (Fig. 2D). DNPME-treated rats were also much more glucose tolerant as reflected by 30–70% reductions in plasma glucose and insulin concentrations at each time-point of an intraperitoneal glucose tolerance test (Fig. 2E–F, S2C–D). DNPME-treated rats also manifested increased whole body insulin responsiveness as reflected by a greater than three fold increase in the glucose infusion rate required to maintain euglycemia during the hyperinsulinemiceuglycemic clamp (Fig. 2G, S2E–G). This increase in insulin-stimulated whole body glucose metabolism in the DNPME-treated rats could be attributed to improvements in both hepatic and peripheral insulin sensitivity (Fig. 2H–I). The increased insulin-stimulated peripheral glucose metabolism was associated with a more than two-fold increase in insulin-stimulated glucose uptake in skeletal muscle (Fig. 2J). These improvements in hepatic and peripheral insulin sensitivity were associated with 40–50% reductions in liver and muscle TAG (Fig. 2K–L) and diacylglycerol (DAG) content (Fig. S2H–K). Consistent with the reduced liver and muscle DAG concentration, we observed reduced protein kinase C (PKC)ε and PKCθ translocation in liver and muscle respectively in DNPME-treated rats (Fig. S2L–M), which is consistent with a role for DAG mediated nPKC activation in causing the liver and muscle insulin resistance (Griffin et al., 1999; Yu et al., 2002; Itani et al, 2002, Samuel et al., 2004; Samuel et al., 2007). In contrast there were no differences in liver or muscle ceramide content, liver glycogen content or any alterations in

plasma adiponectin, FGF-21, and lactate concentrations thus dissociating these factors from DNPME-induced improvements in liver and muscle insulin sensitivity in these animals (Fig. S2N–S). We also examined the effect of DNPME on plasma markers of inflammation (IL-1α, IL-β, IL-2, IL-4, IL-6, IL-10, IL-12, IFNγ, TNFα, GM-CSF), and found no effect of DNPME on any of these cytokines although there was a small reduction in plasma IL-13 concentrations and a trend for reduced plasma RANTES concentration (Fig. S2T).

In order to determine if DNPME treatment reduced hepatic TAG/DAG content by promoting increased hepatic mitochondrial uncoupling *in vivo*, we measured liver-specific rates of oxidative flux pathways and observed a 50% increase in rates of hepatic TCA (V_{TCA}) flux (Fig. 2N) after one and five days of DNPME treatment. This increased hepatic mitochondrial V_{TCA} flux was fueled entirely by increased hepatic fatty acid oxidation flux on day 1 when liver fat content was unchanged between vehicle- and DNPME-treated rats (18.2±1.5 vs. 16.9±2.8 mg/kg, *P*=0.70), but changed to an increase in mostly glucose oxidation, through increased pyruvate dehydrogenase flux (V_{PDH}), on day 5, when liver fat content normalized. This V_{PDH}/V_{TCA} flux observed on day 5 was similar to that observed in the liver of normal chow fed rats, whereas V_{PDH}/V_{TCA} flux on days 0 and 1 was consistent with that observed in high-fat fed rats (Alves et al., 2011). In contrast the ratio of mitochondrial fatty acid oxidation to V_{TCA} flux was unchanged by DNPME treatment in all other tissues including skeletal muscle (Fig. 2O). While these relative flux measurements do not allow us to rule out a small absolute increase in V_{TCA} in peripheral tissues, they are consistent with the hypothesis that the functional effects of DNPME to raise oxygen consumption rate *in vivo* are limited mostly to the liver.

Given these results, in the context of the observed reductions in muscle TAG/DAG content and increases in skeletal muscle insulin sensitivity observed with DNPME treatment we examined whether these effects of DNPME to lower muscle TAG/DAG content might be explained by DNPME-induced reductions in hepatic VLDL production. Consistent with this hypothesis we observed a 50% reduction in hepatic VLDL production with DNPME treatment (Fig. 2M). Taken together these data demonstrate the potential to treat both liver and skeletal muscle insulin resistance by promoting increased hepatic fat oxidation through increased hepatic mitochondrial uncoupling. Consistent with the reduced fasting plasma glucose concentrations and reductions in basal rates of hepatic glucose production measured in DNPME treated rats after 5 days of DNPME treatment, these animals also exhibited a 30% reduction in hepatic pyruvate carboxylase flux (V_{PC}) (Fig. 2P), whereas there was no difference in V_{PC} flux on the first day of DNPME treatment when liver TAG content was unchanged.

Given the effects of DNPME to reduce ectopic lipid content in liver and skeletal muscle and improve whole body insulin sensitivity in both the NAFLD prevention and reversal studies we examined whether DNPME treatment would improve fasting and postprandial plasma glucose and insulin concentration profiles in a rat model of T2D. To evaluate this question we examined the effect of 14 days of DNPME vs. vehicle treatment in a high fat fed/STZ-nicotinamide treated rat model of T2D (Masiello et al., 1998; Reed et al., 2000; Samuel et al., 2004; Samuel et al., 2009). Despite having no difference in body weight or white adipose tissue weight, and consistent with a primarily hepatic uncoupling effect and

unchanged whole-body metabolism (Fig. S3A–B), DNPME treatment normalized fasting plasma glucose and triglyceride concentrations (Fig. 3A–C). DNPME treatment also resulted in a marked improvement in glucose tolerance associated with lower plasma insulin concentrations, reflecting improved whole-body insulin sensitivity (Fig. 3D–E, S3C–D). Finally, and consistent with the results in the other insulin resistant rodent models of NAFLD, DNPME treatment caused a marked reduction in both liver and muscle TAG content (Fig. 3F–G), without any indication of renal or hepatic histopathology (Fig. S1E–F). To further test the assertion that DNPME treatment ameliorates hyperglycemia in a rat model of chronic type 2 diabetes, we performed 5-day DNPME treatment studies on Zucker Diabetic Fatty (ZDF) rats concurrently fed a high fat diet and sucrose supplemented drinking water. Similar to the results in the T2D model previously described, DNPME treatment resulted in reductions in fasting plasma glucose, insulin and liver triglyceride concentrations with no indication of liver or renal dysfunction (Fig. S3G–O).

In order to examine the impact of DNPME on whole body energy expenditure and other metabolic parameters we performed metabolic cage (CLAMS) studies in DNPME and vehicle treated mice. Interestingly we observed no effects of DNPME (5 mg/kg per day) on whole body oxygen consumption, carbon dioxide production, energy expenditure, respiratory quotient, or activity (Fig. S4A–E). Consistent with the rat studies we also observed no effect of DNPME on food intake (Fig. S4F). Taken together these data suggest that DNPME at a dose of 5 mg/kg per day promotes subtle increases in hepatic energy uncoupling that can result in major reductions in liver and muscle fat content with associated reversal of liver and muscle insulin resistance without a major impact on whole body energy expenditure.

It is also possible that low circulating levels of DNP, derived from hepatic conversion of DNPME to DNP by the P450 system, promotes low levels of mitochondrial uncoupling in muscle and other extra-hepatic organs. In order to examine this possibility we assessed the effects of DNPME and DNP on state 4 oxygen consumption *in vitro* and observed an increase in state 4 mitochondrial oxygen consumption of liver but not brain by DNPME, whereas DNP promoted increased state 4 mitochondrial oxygen consumption both tissues in isolated mitochondria in both tissues. In contrast, neither drug uncoupled skeletal or cardiac muscle, or kidney at the respective tissue concentrations measured in the DNPME treatment studies (Fig. S4G–K). These data imply that at the dose of DNPME administered *in vivo*, the mitochondrial uncoupling effect of DNPME appears to be mostly restricted to the liver, and can be attributed to local conversion of DNPME to DNP by the P450 system. These data are consistent with the observed selective effect of DNPME to only increase mitochondrial fat oxidation flux/V_{TCA} flux in liver (Fig. 2P) and the higher DNP concentrations in liver relative to skeletal muscle, heart and brain following DNPME treatment (Fig.4C). While kidney DNP concentrations were similar to liver this could be attributed to the fact that DNP is cleared from the body mostly by renal excretion. It is also possible that there was some renal conversion of DNPME to DNP due to the presence of P450 in the kidney, however, in contrast to liver, we did not observe any effects of DNPME to increase mitochondrial fat oxidation flux/V_{TCA} flux in kidney suggesting minimal effects of DNPME on renal mitochondrial function *in vivo*. In addition we observed no differences in ATP/AMP,

ATP/ADP or NADH/NAD$^+$ ratios in liver and skeletal muscle, or in phosphorylation of hepatic AMP-activated protein kinase (AMPK) or its downstream target acetyl CoA carboxylase (ACC), demonstrating that DNPME is not altering the intracellular energy charge in these tissues at this therapeutic dose (Fig. S4L–R), although we cannot rule out a small effect on peripheral tissues from either local DNPME conversion to DNP, or uncoupling by circulating DNP generated in the liver but released to the systemic circulation.

In order to gain further insights into why DNPME does not result in hyperthermia at similar doses as DNP we measured plasma and tissue levels of DNP and DNPME by LC/MS/MS. We found that dosing rats with DNPME at 5mg/kg by intraperitoneal injection resulted in peak plasma DNP concentrations of ~5 μM and peak liver DNP concentrations of ~8 μM (Fig. 4A–B). DNP concentrations in all tissues were below 10 μM, while DNPME accumulated in WAT but not any other tissue (Fig. 4C–D). In contrast we found that the same dose of DNP (5 mg/kg) resulted in a peak plasma DNP concentration of ~120 μM and a peak DNP liver concentration of ~60 μM (Fig. 4E). In order to determine how these plasma concentrations of DNP compare with toxic levels of DNP we also examined plasma and liver concentrations of DNP at the lowest dose of DNP (25 mg/kg) where systemic toxicities are observed and found peak plasma DNP concentrations to be ~380 μM (Fig. 4F–G). Importantly, a week of DNPME treatment resulted in tissue DNP and DNPME concentrations similar to those following a one-time DNPME injection (Fig. 4H–I). Further kinetics studies would be required to establish conclusively that the improved safety of DNPME versus DNP is purely the result of reduced DNP concentrations with DNPME treatment, but these data are consistent with that hypothesis. Our data suggest that very low intracellular concentrations of DNP, which are more than 75 fold lower than toxic levels of DNP (380 μM) are sufficient to achieve significant liver mitochondrial uncoupling, resulting in reductions in ectopic lipid content and hepatic triglyceride export as well as reversing liver and muscle insulin resistance without resulting in hyperthermia and associated systemic toxicities.

In summary we have demonstrated that DNPME can safely reverse hepatic steatosis, hypertriglyceridemia and insulin resistance in a rat model of NAFLD without inducing hyperthermia and associated hepatic and systemic toxicities. We also found that DNPME reduces fasting plasma glucose concentrations and improves glucose tolerance in two rat models of T2D. Taken together these data demonstrate the potential feasibility of disassociating the toxicity of DNP from its efficacy by altering the pharmacokinetics of DNP metabolism to treat the related epidemics of NAFLD, metabolic syndrome and type 2 diabetes.

Experimental Procedures

General experimental procedures for chemical synthesis

Chemicals were obtained from commercial sources and used as received, unless noted otherwise. In particular, 2,4-Dinitrophenol (DNP; **1**) was purchased from MP Biomedicals, 2,4-dinitrophenyl methyl ether (DNPME; **2**) from Alfa Aesar, and 1-chloro- 2,4-

dinitrobenzene-d3 (**3**) from C/D/N Isotopes. For detailed information on the synthesis and analysis of the novel compounds, please see the Supplemental Experimental Procedures.

Screening of candidate compounds

To screen candidate compounds, the compounds' ability to raise oxygen consumption rates *in vivo* was assessed using the Seahorse Extracellular Flux Analyzer (Seahorse Bioscience). Primary hepatocytes were isolated by the Yale Liver Center as previously described (Neufeld, 1997) and plated on a collagen-coated 24-well plate (Seahorse Bioscience). After a 6-hour incubation, cells were transferred to the Seahorse XF Analyzer for measurement of oxygen consumption rate. Basal oxygen consumption was measured, then sequential additions of DNP (positive control) or the candidate compounds raised the concentration of the putative uncoupler to 10, 100, 500, and 1000 μM. Absolute oxygen consumption rates were normalized to the oxygen consumption rate measured before the first addition of uncoupler.

Animals

All animals were male. C57BL6J mice were ordered from Jackson Laboratories at 25 g. Sprague-Dawley and Zucker Diabetic Fatty rats weighing 300–400 g were ordered from Charles River Laboratories. Animals were allowed to acclimate for 1–3 weeks before use. All protocols were approved by the Yale University School of Medicine Animal Care and Use Committee. Further information on surgical procedures, housing, and diet are included in the Supplementary Experimental Procedures.

Toxicity studies

For the acute toxicity studies, rats were treated with an IP injection of DNPME in 100% DMSO at doses 1, 2.5, 5, 10, 25, 50, 100, and 200 mg/kg body weight. Rectal temperature was measured with a microprobe thermometer (Physitemp Instruments) at intervals up to 2 hours after injection of the drug. Rectal temperature was measured weekly in a separate group of rats injected daily with DNPME or vehicle for 6 weeks. A separate group of rats were injected with increasing doses of DNP or DNPME in 100% DMSO to determine the 50% lethal dose (LD_{50}). The 50% lethal dose was taken to be the dose at which 50% of rats died within 24 hours of treatment.

To assess renal and hepatic toxicity, a group of catheterized rats was treated with an intraperitoneal (IP) injection of DMSO vehicle or 1, 2.5, 5, 10, 25 50, 100, or 200 mg/kg DNPME in DMSO daily. After five days, the rats were sacrificed and plasma obtained from the intravenous catheter. The COBAS Mira Plus (Roche Diagnostics) was used to measure plasma alanine aminotransferase (ALT), aspartate aminotransferase (AST), and blood urea nitrogen (BUN). Plasma creatinine was measured by liquid chromatography/mass spectrometry/mass sprectrometry (LC/MS/MS). 24 hour creatinine clearance was measured by housing rats treated with DNPME or vehicle in metabolic cages for 24 hours, collecting the urine, and measuring urine creatinine concentration by LC/MS/MS.

Histology studies

Liver and kidney samples were prepared and stained with hematoxylin & eosin by the Yale Research Histology core, and analyzed as described (Kleiner et al., 2005).

Glucose tolerance tests

Following an overnight fast, rats with a jugular venous line were injected with a 1 g/kg intraperitoneal bolus of 50% dextrose. Plasma glucose following the injection was measured enzymatically on the YSI Life Sciences 2700 Select Biochemistry Analyzer, and plasma insulin was measured by radioimmunoassay by the Yale Diabetes Research Core. Area under the curve was measured from time point A to subsequent time point B according to the following formula:

$$AUC_{A \to B} = \frac{1}{2}(Plasma glc_A + Plasma glc_B) \times (Time_B - Time_A)$$

The total area under the curve was calculated by adding the area under the curve of each of the subsequent time periods. The insulin area under the curve was calculated in the same way.

Basal and insulin-stimulated glucose turnover studies

Hyperinsulinemic-englycemic clamps were performed and basal and insulin-stimulated glucose turnover were measured using [6,6]^{2}H$_2$ glucose as previously described (Erion et al., 2013). To measure insulin-stimulated glucose uptake in heart and quadriceps muscle, [^{14}C]2-deoxyglucose was injected at the conclusion of the clamp, and tissues processed as described previously (Samuel et al., 2007).

Protein kinase ε and θ translocation

Protein kinase (PKC)ε translocation in liver and PKCθ translocation in muscle from 6-hour fasted rats in the NAFLD treatment study were measured by Western blot as previously reported (Choi et al., 2007).

Lipid concentration assays

Triacylglycerol (TAG) in liver and quadriceps muscle were extracted by the method of Bligh and Dyer (1959) and measured spectrophotometrically with Diagnostic Chemicals triglyceride reagent (Diagnostic Chemicals Ltd. [DCL]). Liver and quadriceps diacylglycerol (DAG) were extracted by homogenization in a buffer containing 20mM Tris-HCl, 1mM EDTA, 0.25mM EGTA, 250mM sucrose, 2mM phenylmethylsulfonyl fluoride, and a protease inhibitor mixture (Roche). The cytosolic fragment was isolated from the supernatant after high-speed centrifugation for 1 hour. DAG and ceramide content was measured by LC/MS/MS (Yu et al., 2002). Liver triglyceride export was measured as we have described (Lee et al., 2011).

Measurement of liver glycogen content

Hepatic glycogen content was assessed by amyloglucosidase digestion using the method of Passonneau and Lauderdale (1974).

Assessment of plasma metabolites, adipocytokines and inflammatory markers

Plasma concentrations of twelve inflammatory markers were measured by ELISA (QIAGEN). Adiponectin was measured by radioimmunoassay by the Yale Diabetes Research Center Physiology Core. Lactate was measured by COBAS, and FGF-21 by ELISA (Millipore).

Assessment of basal metabolism in mice

Mice were studied during daily IP injections of 5 mg/kg DNPME or vehicle. Comprehensive Animal Metabolic Monitoring System (Columbus Instruments) was used to measure oxygen uptake and carbon dioxide production, daily caloric intake and energy expenditure, respiratory exchange ratio, and activity throughout the day.

Evaluation of hepatic flux rates in rats

To measure liver-specific flux through the TCA cycle, we performed a steadystate infusion of [3-^{13}C] lactate [5 min prime 120 μmol/(kg-min), 115 min continuous infusion 40 μmol/(kg-min)] and [^{3}H] glucose (44 μmol/min). At 120 min, plasma and livers were isolated, and hepatic fluxes were measured by nuclear magnetic resonance (NMR) and LC/MS/MS as described in the Supplemental Experimental Procedures.

Measurement of plasma and tissue DNP and DNPME concentrations

We measured DNP and DNPME concentrations using LC/MS/MS. Details can be found in the Supplementary Experimental Procedures.

Kinetics studies

To evaluate the kinetics of DNP and DNPME, a 5 mg/kg dose of DNPME was injected at time zero. Rats were sacrificed at 1, 2, 4, 6, 12, and 24 hours to isolate the liver, and plasma was drawn through a venous catheter at each time point. Plasma and liver concentrations of DNP and DNPME were measured by LC/MS/MS.

To compare tissue concentrations of DNPME and DNP with various injection protocols, separate groups of rats (n=4 per group) were treated with 5 mg/kg DNPME, 5 mg/kg DNP, or 25 mg/kg DNP. The DNPME injected rats were sacrificed 4 hours after the last injection, while the DNP injected rats were sacrificed 1 hour after the last injection, times which in the previous kinetics studies had been determined to represent the peak plasma concentrations of DNP with the respective injections. Plasma and tissues were isolated.

Mitochondrial respiration studies

Isolated mitochondria from liver and brain of overnight fasted rats were prepared (Andrews et al., 2008), and respiration measured on the Seahorse XF Analyzer. Additional details may be found in the Supplemental Experimental Procedures.

Assessment of tissue energetics

To measure tissue ATP, ADP, AMP, NADH, and NAD$^+$ concentration, rats were sacrificed by decapitation to allow the fastest possible tissue isolation, and metabolites of interest were extracted and measured by LC/MS/MS as described in the Supplemental Experimental Procedures.

Statistical analysis

All data are expressed as mean ± SEM. Significance was determined using the two-tailed unpaired Student's t-test, or, if indicated, by the two-tailed paired Student's t-test or by ANOVA. Differences with P-value less than 0.05 were considered significant.

Supplementary Material

Refer to Web version on PubMed Central for supplementary material.

Acknowledgments

References

Alves TC, Befroy DE, Kibbey RG, Kahn M, Codella R, Carvalho RA, Petersen KF, Shulman GI. Regulation of hepatic fat and glucose oxidation in rats with lipid-induced insulin resistance. Hepatology. 2011; 53:20–27. [PubMed: 21618566]

Andrews ZB, Liu Z-W, Walllingford N, Erion DM, Borok E, Friedman JM, Tschöp MH, Shanabrough M, Cline G, Shulman GI, et al. UCP2 mediates ghrelin's action on NPY/AgRP neurons by lowering free radicals. Nature. 2008; 454:846–851. [PubMed: 18668043]

Baffy G, Brunt EM, Caldwell SH. Hepatocellular carcinoma in non-alcoholic fatty liver disease: an emerging menace. J. Hepatol. 2012; 56:1384–1391. [PubMed: 22326465]

Bligh EG, Dyer WJ. A rapid method of total lipid extraction and purification. Can J Biochem Physiol. 1959; 37:911–917. [PubMed: 13671378]

Choi CS, Savage DB, Abu-Elheiga L, Liu Z-X, Kim S, Kulkarni A, Distefano A, Hwang Y-J, Reznick RM, Codella R, et al. Continuous fat oxidation in acetyl-CoA carboxylase 2 knockout mice increases total energy expenditure, reduces fat mass, and improves insulin sensitivity. Proc. Natl. Acad. Sci. U.S.a. 2007; 104:16480–16485. [PubMed: 17923673]

Erion DM, Popov V, Hsiao JJ, Vatner D, Mitchell K, Yonemitsu S, Nagai Y, Kahn M, Gillum MP, Dong J, et al. The role of the carbohydrate response element-binding protein in male fructose-fed rats. Endocrinology. 2013; 154:36–44. [PubMed: 23161873]

Griffin ME, Marcucci MJ, Cline GW, Bell K, Barucci N, Lee D, Goodyear LJ, Kraegen EW, White MF, Shulman GI. Free fatty acid-induced insulin resistance is associated with activation of protein kinase C theta and alterations in the insulin signaling cascade. Diabetes. 1999; 48:1270–1274. [PubMed: 10342815]

Itani SI, Ruderman NB, Schmieder F, Boden G. Lipid-induced insulin resistance in human muscle is associated with changes in diacylglycerol, protein kinase C, and IkappaB-alpha. Diabetes. 2002; 51:2005–2011. [PubMed: 12086926]

Lee H-Y, Birkenfeld AL, Jornayvaz FR, Jurczak MJ, Kanda S, Popov V, Frederick DW, Zhang D, Guigni B, Bharadwaj KG, et al. Apolipoprotein CIII overexpressing mice are predisposed to diet-induced hepatic steatosis and hepatic insulin resistance. Hepatology. 2011; 54:1650–1660. [PubMed: 21793029]

Masiello P, Broca C, Gross R, Roye M, Manteghetti M, Hillaire-Buys D, Novelli M, Ribes G. Experimental NIDDM: development of a new model in adult rats administered streptozotocin and nicotinamide. Diabetes. 1998; 47:224–229. [PubMed: 9519717]

Neufeld DS. Isolation of rat liver hepatocytes. Methods Mol. Biol. 1997; 75:145–151. [PubMed: 9276266]

Passonneau JV, Lauderdale VR. A comparison of three methods of glycogen measurement in tissues. Anal. Biochem. 1974; 60:405–412. [PubMed: 4844560]

Petersen KF, Dufour S, Befroy D, Lehrke M, Hendler RE, Shulman GI. Reversal of nonalcoholic hepatic steatosis, hepatic insulin resistance, and hyperglycemia by moderate weight reduction in patients with type 2 diabetes. Diabetes. 2005; 54:603–608. [PubMed: 15734833]

Reed MJ, Meszaros K, Entes LJ, Claypool MD, Pinkett JG, Gadbois TM, Reaven GM. A new rat model of type 2 diabetes: the fat-fed, streptozotocin-treated rat. Metab. Clin. Exp. 2000; 49:1390–1394. [PubMed: 11092499]

Samuel VT, Shulman GI. Mechanisms for insulin resistance: common threads and missing links. Cell. 2012; 148:852–871. [PubMed: 22385956]

Samuel VT, Beddow SA, Iwasaki T, Zhang X-M, Chu X, Still CD, Gerhard GS, Shulman GI. Fasting hyperglycemia is not associated with increased expression of PEPCK or G6Pc in patients with Type 2 Diabetes. Proc. Natl. Acad. Sci. U.S.a. 2009; 106:12121–12126. [PubMed: 19587243]

Samuel VT, Liu Z-X, Wang A, Beddow SA, Geisler JG, Kahn M, Zhang X-M, Monia BP, Bhanot S, Shulman GI. Inhibition of protein kinase Cepsilon prevents hepatic insulin resistance in nonalcoholic fatty liver disease. J. Clin. Invest. 2007; 117:739–745. [PubMed: 17318260]

Samuel VT, Liu Z-X, Qu X, Elder BD, Bilz S, Befroy D, Romanelli AJ, Shulman GI. Mechanism of hepatic insulin resistance in non-alcoholic fatty liver disease. J. Biol. Chem. 2004; 279:32345–32353. [PubMed: 15166226]

Shulman GI. Cellular mechanisms of insulin resistance. J. Clin. Invest. 2004; 106:171–176. [PubMed: 10903330]

Tainter ML, Cutting WC, Stockton AB. Use of Dinitrophenol in Nutritional Disorders : A Critical Survey of Clinical Results. Am J Public Health Nations Health. 1934; 24:1045–1053. [PubMed: 18014064]

White DL, Kanwal F, El-Serag HB. Association between nonalcoholic fatty liver disease and risk for hepatocellular cancer, based on systematic review. Clin. Gastroenterol. Hepatol. 2012; 10:1342–1359. e1342. [PubMed: 23041539]

Yu C, Chen Y, Cline GW, Zhang D, Zong H, Wang Y, Bergeron R, Kim JK, Cushman SW, Cooney GJ, et al. Mechanism by which fatty acids inhibit insulin activation of insulin receptor substrate-1 (IRS-1)-associated phosphatidylinositol 3-kinase activity in muscle. J. Biol. Chem. 2002; 277:50230–50236. [PubMed: 12006582]
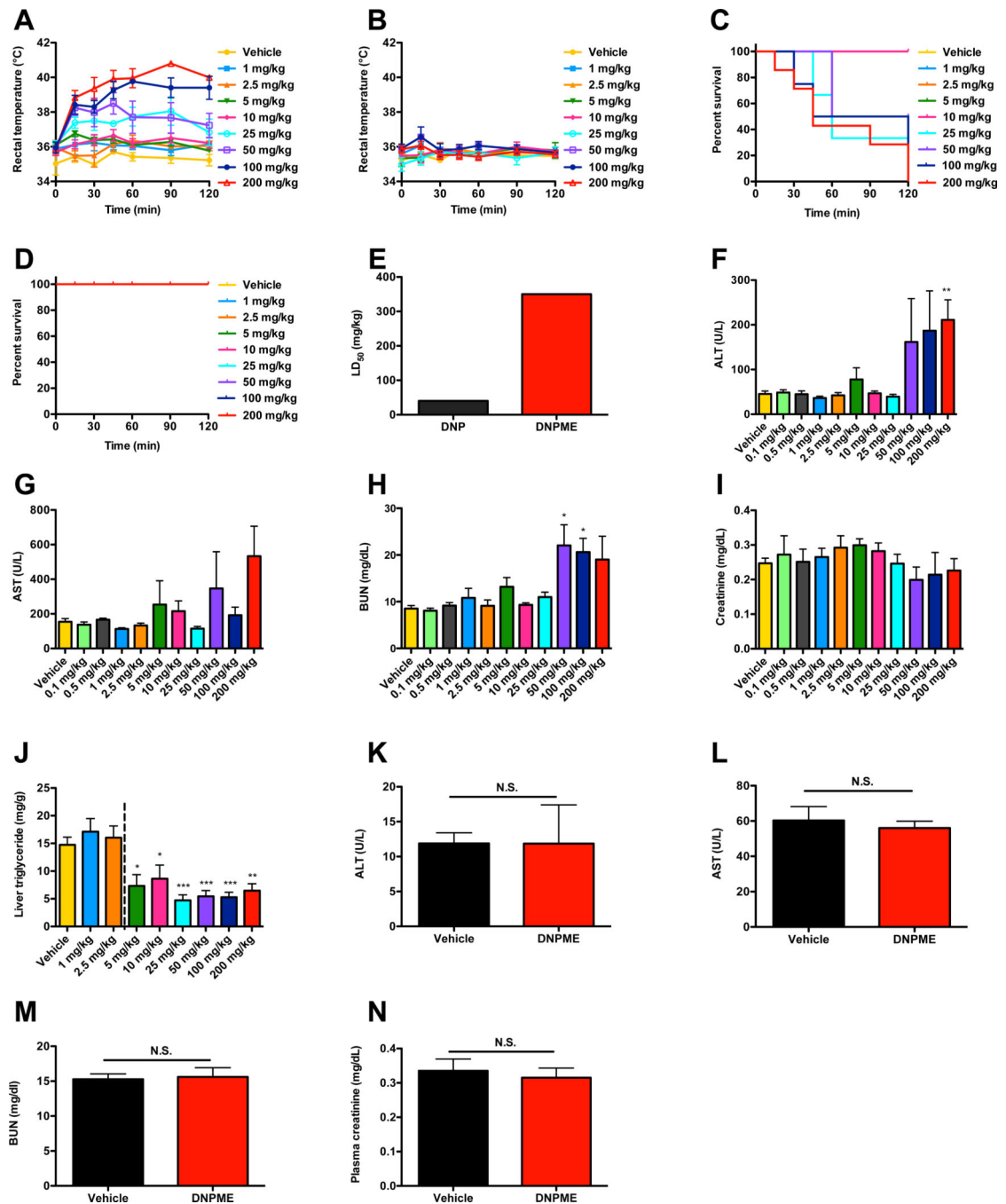
Fig. 1.
Safety and efficacy profile of DNPME compared to DNP in rats. (A), (B) Rectal
temperature following a single IP injection of DNP or DNPME. (C), (D) Survival acutely
following treatment with DNP or DNPME. (E) LD$_{50}$ of DNP and DNPME. (F)–(I) Plasma
ALT, AST, BUN, and creatinine after 5 days of daily treatment with DNPME or vehicle in
chow-fed rats. (J) Liver TAG in overnight-fasted rats after 5 days of daily treatment with
DNPME during high fat/sucrose water feeding. (K)–(N) ALT, AST, BUN, and creatinine

after 6 weeks of daily DNPME treatment (5 mg/kg) in chow-fed rats. For all panels, n=4–6 per dose, and data are represented as mean ± S.E.M. See also Fig. S1.
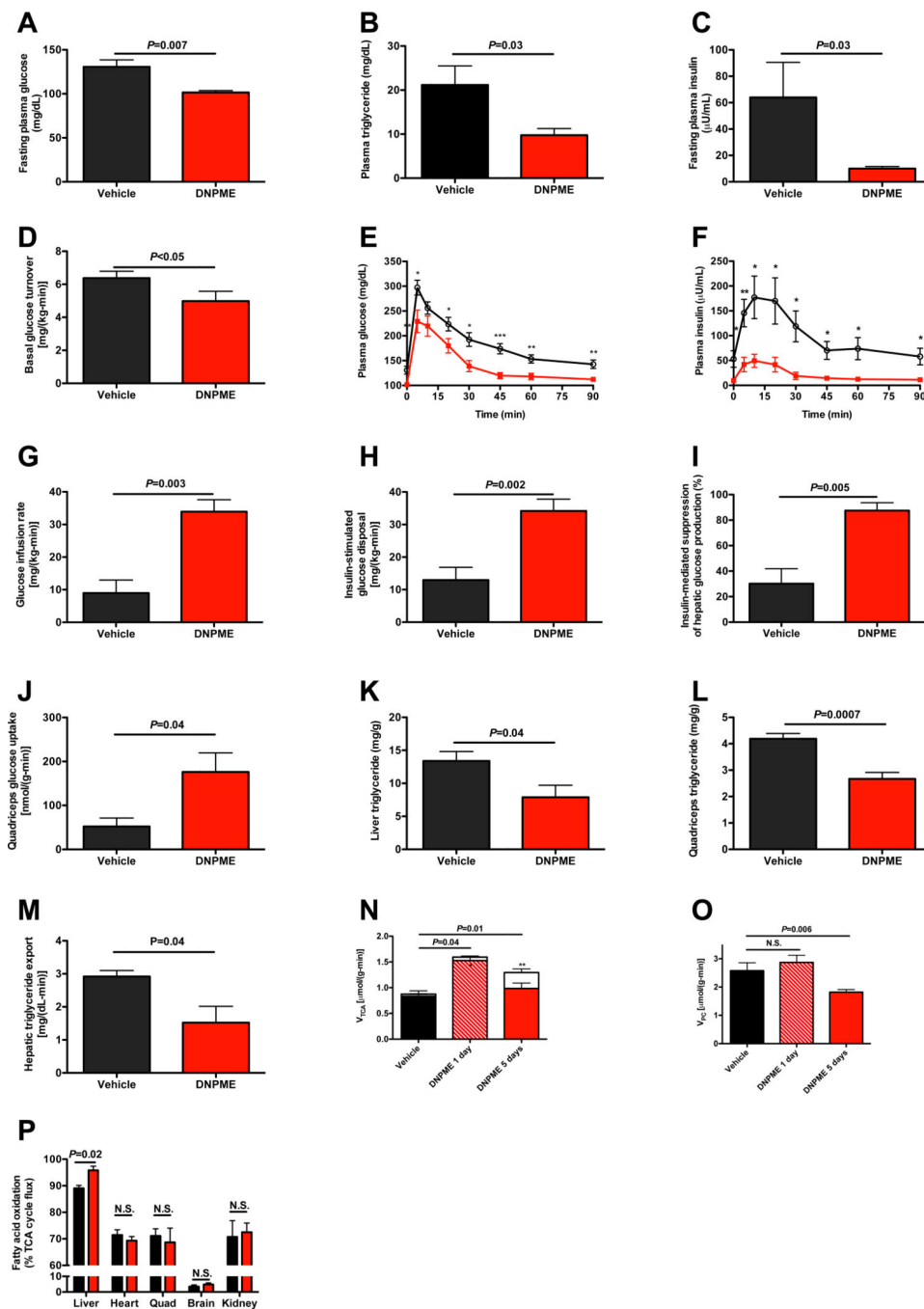
Fig. 2.
DNPME reverses NAFLD, hypertriglyceridemia as well as liver and muscle insulin resistance in rats previously fed high fat diet and sucrose water for 2 weeks, then treated with 5 mg/kg DNPME per day daily for 5 days. (A)–(C) Fasting plasma glucose, triglyceride, and insulin. (D) Basal glucose turnover. (E), (F) Plasma glucose and insulin during an intraperitoneal glucose tolerance test. Black circles = vehicle treated, red squares = DNPME treated. *$P<0.05$, **$P<0.01$, ***$P<0.001$. (G) Glucose infusion rate to maintain euglycemia during the hyperinsulinemic-euglycemic clamp. (H) Insulin-stimulated glucose

metabolism. (I) Insulin-mediated suppression of hepatic glucose production. (J) Insulin-stimulated glucose uptake in quadriceps. (K), (L) Liver and quadriceps TAG. (M) Liver VLDL production. (N) Liver TCA cycle flux (sum of red and white bars) and substrate contributions (fatty acid oxidation, solid bar; flux through PDH, white bar) to the TCA cycle. In panels (N) and (O), n=3 vehicle treated, 3 1 day DNPME treated, and 6 5 days DNPME treated. (O) Fatty acid oxidation relative to V_{TCA} in 1 day DNPME or vehicle treated rats (n=3). (P) Hepatic flux through pyruvate carboxylase. Rats were fasted overnight (16 hours) prior to each of these studies. Unless otherwise specified, n=5–8 per group. Data are represented as mean ± S.E.M. See also Fig. S2.
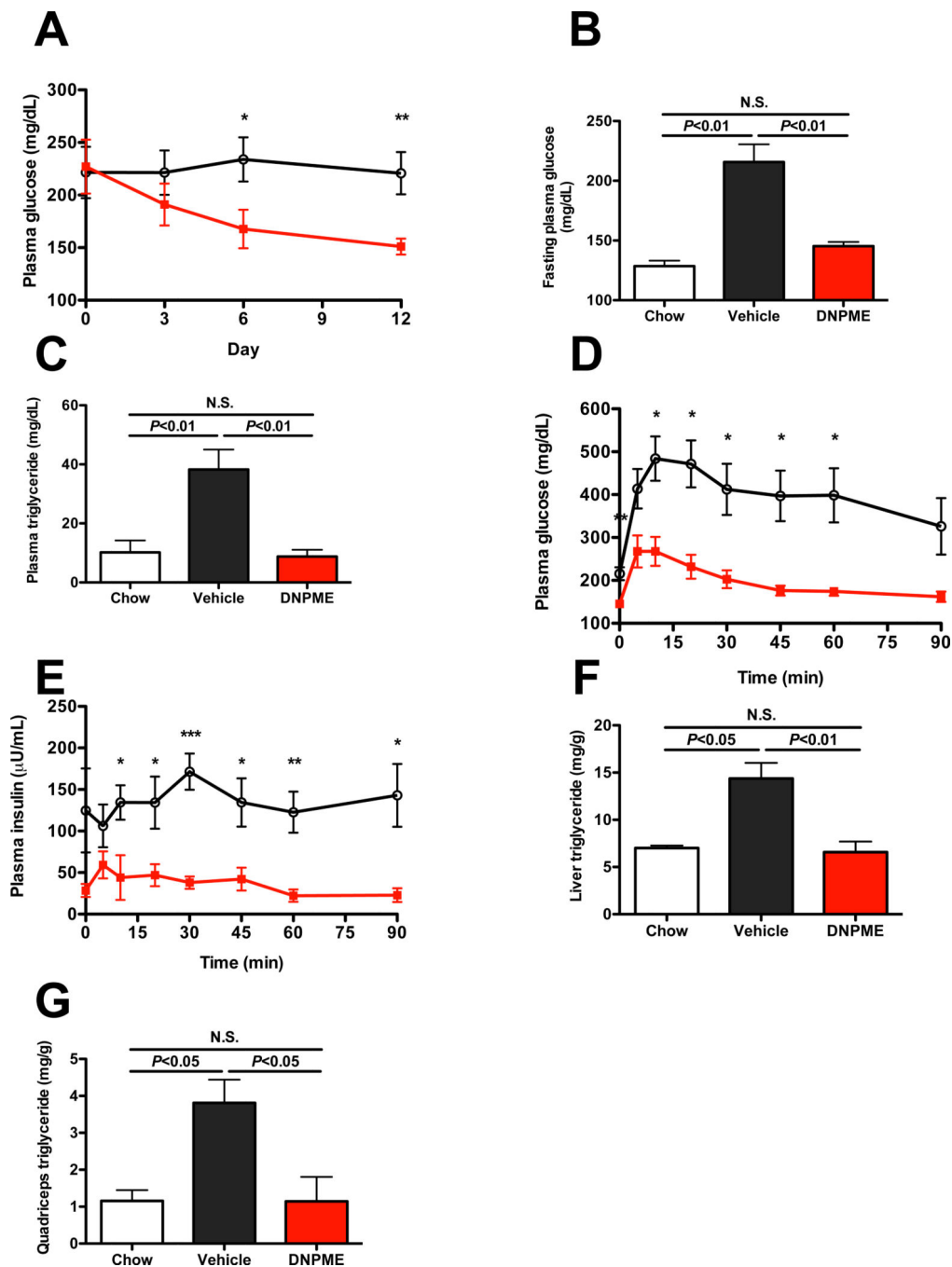
Fig. 3.
Daily DNPME (5 mg/kg) reverses hyperglycemia, hypertriglyceridemia and hepatic
steatosis in a low dose streptozotocin treated/3 day high fat fed rat model of type 2 diabetes
and NAFLD. (A) Random plasma glucose concentrations during DNPME treatment. (B),
(C) Fasting plasma glucose and TAG concentrations. (D), (E) Plasma glucose and insulin
concentrations in an intraperitoneal glucose tolerance test. (F), (G) Liver and quadriceps
TAG. For all panels, n=4–7 per group. In all cases, rats were fasted overnight before the

study. Data are represented as mean ± S.E.M. In the panels comparing chow, vehicle-treated, and DNPME-treated rats, comparisons were by ANOVA. See also Fig. S3.
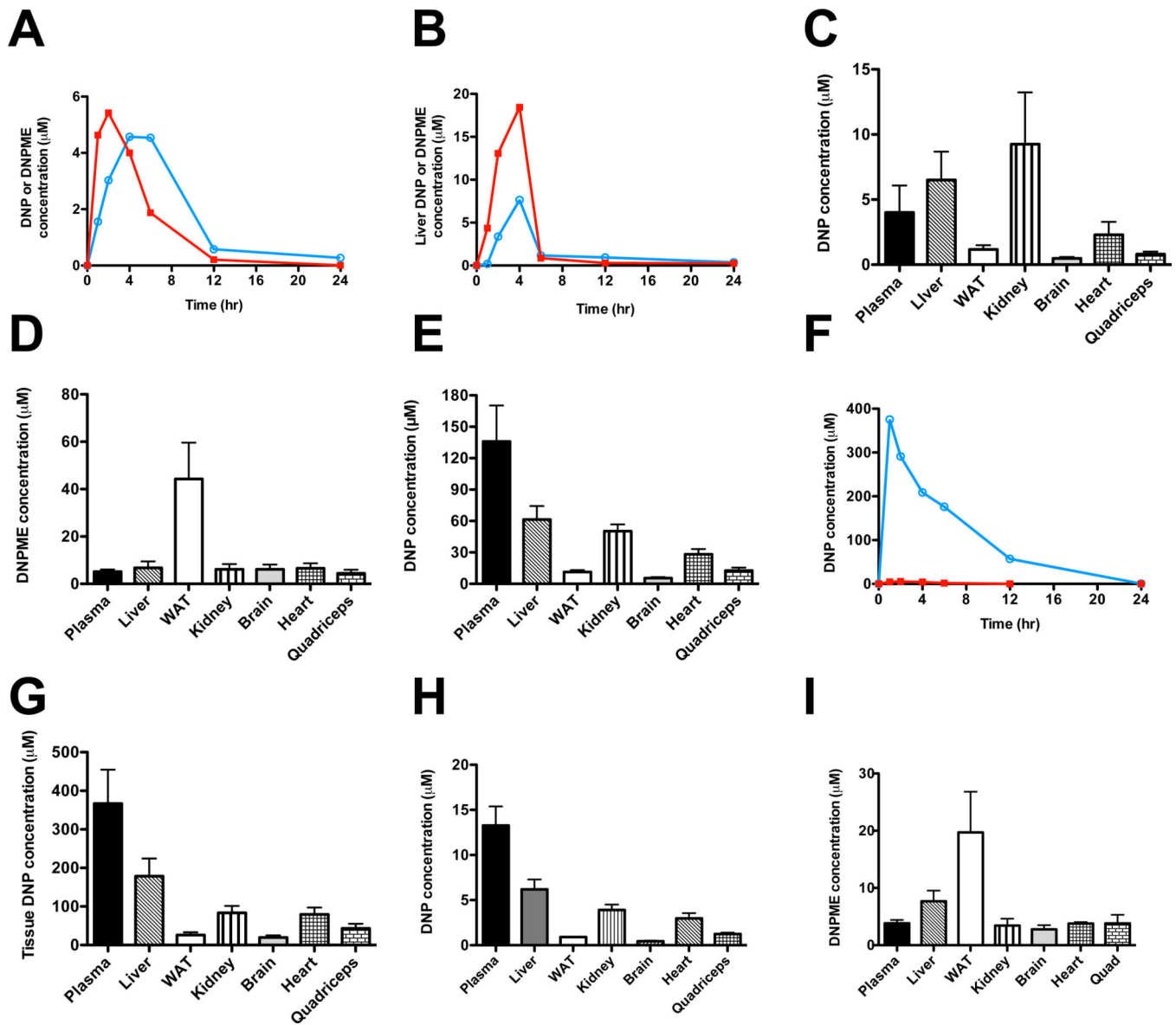
Fig. 4.
Plasma and tissue kinetics of DNP and DNPME metabolism in chow-fed Sprague-Dawley rats. (A) Plasma DNP and DNPME concentration after an intraperitoneal injection of DNPME (5 mg/kg) at time zero. (B) Liver DNP and DNPME concentration after an injection of DNPME (5 mg/kg). In panels A and B, red squares = DNPME, blue circles = DNP; each timepoint represents an individual animal. (C), (D) Tissue concentrations of DNP and DNPME 4 hours after an injection of DNPME (5 mg/kg). (E) Tissue concentration of DNP 1 hour after an injection of DNP (5 mg/kg). (F) Plasma DNP concentration after an injection of DNP (25 mg/kg, blue circles) or DNPME (5 mg/kg, red squares). Each timepoint represents an individual animal. (G) Plasma and tissue concentrations of DNP after injection of DNP (25 mg/kg). Tissues were isolated 1 hour after DNP injection. (H), (I) DNP and DNPME concentrations in tissues after 7 days of daily DNPME injections (5

mg/kg per day). Unless otherwise noted, n=4 per group. Data are expressed as mean ± S.E.M. See also Fig. S4.